

## Perspective Article

## Dual-cured thermosets from glycidyl methacrylate obtained by epoxy-amine reaction and methacrylate homopolymerization

Adrià Roig<sup>a</sup>, Xavier Ramis<sup>b</sup>, Silvia De la Flor<sup>c</sup>, Àngels Serra<sup>a,\*</sup><sup>a</sup> Analytical and Organic Chemistry Dpt., Universitat Rovira i Virgili, C/ Marcel·lí Domingo s/n Edif. N4, 43007 Tarragona, Spain<sup>b</sup> Thermodynamics Laboratory, ETSEIB Universitat Politècnica de Catalunya, Av. Diagonal, 08028 Barcelona, Spain<sup>c</sup> Dept. of Mechanical Engineering, Universitat Rovira i Virgili, Av. Països Catalans, 26, 43007 Tarragona, Spain

## ARTICLE INFO

## Keywords

Dual-curing  
Thermosets  
Click chemistry  
Epoxy-amine  
Radical homopolymerization

## ABSTRACT

Dual-curing is a processing technology based in the combination of two polymerization processes and the proper selection of the formulation. This methodology allows the preparation of intermediate materials with tailored characteristics, which can be viscous-liquids or rubbery solids according to their application. Once applied, the second stage is performed leading to a high crosslinked network. Usually, different monomers are involved, and unreacted monomer are still present in the intermediate material. This monomer experiments polymerization during the second step, but it can drip or be exuded during storage. In the present work, a commercial monomer, glycidyl methacrylate has been selected, because of the presence in the same molecule of an epoxide group, which can react with amines in the first stage of the dual-curing, and a methacrylate group that can be thermally or photochemically homopolymerized to complete the curing process. Diglycidylether of bisphenol A has been added to obtain a gelled intermediate material. The evolution of both curing steps has been studied by DSC and FTIR. The stability of the intermediate material has been confirmed and the characteristics of intermediate and final material have been evaluated by TGA and DMTA.

## 1. Introduction

Nowadays thermosets are an important type of industrial materials due to their wide range of applications in several sectors such as coatings [1], automobile [2] or optoelectronic industry [3]. The preparation of these cross-linked materials involves irreversible curing processes that must be very well-controlled to produce components with the required characteristics and shapes. In this field, dual-curing has arisen as a promising synthetic methodology to obtain thermosets in a well-controlled manner. This procedure consists in two different polymerization processes that can take place sequentially or simultaneously and can be triggered by different stimuli i.e. temperature or UV-light [4]. Sequential dual curing allows to obtain partially cured materials in a first stage that can be easily stored or just sent for further processing to obtain a fully cured polymer with higher performance once the second polymerization is completed. The characteristics of the intermediate materials can be modulated and depend on the formulation composition which in turn, defines the extension of the first and second curing stages. The intermediate materials can be viscous liquids, with

adhesive properties, or conformable solid materials, which after performing the second step will be converted into hard thermosets.

The sequentiality and the control of the intermediate characteristics are based on the selection of the curing reactions, the composition of the formulation and the tuning of the curing parameters like time or temperature of the process and in some cases the use of an adequate catalyst [5]. Dual-curing processing presents several advanced applications in shape memory polymers [6–9], adhesive coatings [10,11], lithography [9,12], holography [13,14], photopatterning [15] or dental materials [16] among many others.

To achieve sequential dual curing processes, “click chemistry” is a great tool because it provides selectivity, great kinetic control, high yields in mild reaction conditions, and can be performed in air atmosphere [17–20]. Among all the possible reactions that are included in this type of chemistry, one of the most used in the synthesis of thermosets is the epoxy-amine reaction as it can be carried out at low temperatures in case of using aliphatic amines as curing agents. Many researchers used this reaction as a first step in dual curing schemes. Konuray et al. employed a two-stage curing process in which the digly-

\* Corresponding author.

E-mail address: [angels.serra@urv.cat](mailto:angels.serra@urv.cat) (À. Serra)

glycidyl ether of bisphenol A (DGEBA) and an aliphatic amine are involved in the first curing step to synthesize a wide range of intermediate materials, with different properties depending on the composition of the formulation, whereas a homopolymerization of the remaining epoxy groups initiated by a latent imidazole catalyst constituted the second stage [21]. Similarly, Morancho et al. described the dual-curing of off-stoichiometric diethylenetriamine-diglycidyl ether of bisphenol A using tertiary amine as initiator for high temperature homopolymerization of the epoxy excess [22]. After the first curing stage, intermediate materials showed a high latency and could be safely stored for long time, since in addition of the kinetic control in the initiation of the second stage, vitrification of the intermediate material helps to improve their storability, if storage temperatures are lower than the  $T_g$ . Furthermore, the same group also reported a new family of dual-cured thermosets based on commercial amine-epoxy formulations with two amines of different reactivity and rigidity reaching promising materials for applications such as adhesives or smart materials [23].

As said, the second curing stage is also a very important step to produce the fully cured material because it will generate the final network in the thermoset and subsequently, determine the final characteristics. This reaction can be activated by UV-light or thermally, depending on the type of reactive groups and the chemistry involved, having both processes their advantages and drawbacks. From the point of view of energy saving and technical easiness, photoirradiation is very advantageous, but its application is reduced to thin layers and flat shapes that can be fully illuminated without shadowy parts [24]. Thermal activation is better for thick and complex shaped samples because of its uniformity, but high temperatures in ovens and long curing times are needed. In addition, vitrification of the final material must be avoided and from this point of view, thermal activation is more convenient.

Taking all of this into account, in the present article, we report the preparation and characterization of a new dual-curing system based on the epoxy and methacrylate groups of a commercially available compound, glycidyl methacrylate (GMA). A stoichiometric epoxy-amine reaction will be used as the first curing stage and a radical homopolymerization of the methacrylate groups in both thermal and UV-curing conditions as the second curing stage. The addition of DGEBA to the formulation has also been explored to achieve gelation during the first step. As far as we know, this dual curing system has not been previously described in the literature, and the combination of both polymerization mechanism can open broad industrial applications. However, Mustata et al. reported the curing of GMA/DGEBA mixtures with adducts of Diels-Alder reaction of rosin acids derivatives and maleic anhydride, being the first step the thermal curing of methacrylates and the second, the reaction of epoxides with acids and anhydrides [25]. The most valuable advancement of the present study relies on the fact that no unreacted monomers will be present after the first step avoiding their possible dripping or exudation in the conformation or processing of the intermediate material, which is a great advantage in its final application. In addition, this novel curing system has great versatility as different excesses of diepoxide can be added to modify not only the characteristics of the intermediate material, but also of the final material. Of course, mono or multifunctional methacrylates could also be added to the formulation to adapt the properties of the materials, although in the latter case there will be unreacted monomer in the intermediate material. Thermal and photoinitiated homopolymerization of the methacrylate moieties have been studied in order to compare the characteristics of the final materials.

The evolution of both curing stages, the conversion achieved and the latency after the first stage have been evaluated by calorimetry and FTIR spectroscopy and the gelation time during epoxy-amine condensation by rheology. The materials obtained have been characterized by calorimetric, thermomechanical, and thermogravimetric analyses.

## 2. Experimental part

### 2.1. Materials

Glycidyl methacrylate (GMA) was supplied by Miwon. Diethylenetriamine (DETA, 20.63 g/eq), isophorone diamine (IPDA, 42.58 g/eq), tris(2-aminoethyl)amine (TREN, 24.37 g/eq) and 2,2-dimethoxy-2-phenylacetophenone (DMPA) were supplied by Sigma Aldrich and used without further purification. Jeffamine D400 (JEFFA, 115 g/eq) was provided by Huntsman Corporation. Diglycidyl ether of bisphenol A (DGEBA, 172 g/eq) was supplied by Hexion Specialty Chemicals and dried in vacuum for 2 h at 80 °C before use and the peroxidic radical initiator 1,1-di(t-amyloxy)-cyclohexane (Luperox 531 M60) was kindly supplied by ARKEMA.

### 2.2. Sample preparation

Formulations of GMA were prepared in 5 mL vials in approximately 1 g batches were 1% w/w of Luperox (to GMA) for thermal acrylate homopolymerization or 5% w/w of DMPA (to GMA) for photoinitiated systems were weighted. Then, GMA and the stoichiometric amount of amine (IPDA, JEFFA, TREN or DETA) was added. The mixtures were vigorously and manually stirred at room temperature and then immediately analysed.

Formulations of GMA with DGEBA were prepared in 5 mL vials in 1–2 g batches were 1% w/w of Luperox (to GMA) and 5% w/w of DMPA (to GMA) were weighted for thermal and photoinitiated methacrylate homopolymerization, respectively. Then, DGEBA and the corresponding amount of GMA were added using the calculated molar ratio between DGEBA and GMA ( $n_{DGEBA}/m_{GMA} = 0.4$ ). Finally, the stoichiometric amount of amine (IPDA, JEFFA, TREN or DETA) was added. The reactive mixtures were homogenised at room temperature by manual stirring and then immediately analysed.

The formulations prepared with only GMA were coded as G\_X\_Y and the formulations containing DGEBA as GDG\_X\_Y, where, in both cases, X indicates the amine used and Y the initiator selected for the second stage of the dual process. As an example, GDG\_DETA\_Lup is a formulation in which GMA and DGEBA are in the mixture, DETA is the amine used and the second stage was initiated by 1% w/w of Luperox. Table 1 shows the composition of the different formulations studied.

Fully cured samples for dynamomechanical (DMA) and thermogravimetric (TGA) analyses were prepared in an open mould, with dimensions of  $1.5 \times 5 \times 15 \text{ mm}^3$ , made of metal and covered with PTFE to avoid the formation of bubbles and to facilitate the samples release. The liquid formulations were poured into the mould and kept in an oven at 45 °C for 4.5 h (stage 1), and cured at 120 °C during 1.5 h and post-cured at 150 °C and 200 °C during 1 h and 1.5 h, respectively in the case of Luperox-based compositions, and 1.5 min under UV-light on both sides for DMPA formulations (stage 2). These curing times were optimized according to Fourier transform infrared spectroscopy (FTIR) and differential scanning calorimetry (DSC). The samples were polished with sandpaper to obtain uniform final dimensions.

### 2.3. Characterization techniques

DSC analyses were carried out on a Mettler DSC-821 instruments calibrated using indium (heat flow calibration) and zinc (temperature calibration) standards. Samples of approximately 8–10 mg were placed in aluminium pans with pierced lids and analysed in nitrogen atmosphere with a gas flow of 50 cm<sup>3</sup>/min. Dynamic studies between 30 and 250 °C with heating rate of 10 °C/min were performed to characterize the curing process and to measure the final glass transition temperature ( $T_g$ ). Dynamic curing tests were also performed with heating rates of 2, 5, 10 and 20 °C/min to determine the kinetic parameters. The reaction

**Table 1**  
Composition of the dual formulations prepared.

Sample	GMA (wt%)	DGEBA (wt%)	IPDA (wt%)	JEFFA (wt%)	TREN (wt%)	DETA (wt%)	Lup. (wt%)	DMPA (wt%)
G_IPDA_Lup	76.3	–	22.9	–	–	–	0.8	–
G_JEFFA_Lup	56.6	–	–	42.8	–	–	0.6	–
G_TREN_Lup	84.6	–	–	–	14.6	–	0.8	–
GDG_DETA_Lup	43.0	45.3	–	–	–	11.2	0.5	–
GDG_DETA_DMPA	42.3	44.5	–	–	–	11.1	–	2.1
G_DETA_Lup	86.5	–	–	–	–	12.6	0.9	–
G_DETA_DMPA	83.6	–	–	–	–	12.2	–	4.2

enthalpy ( $\Delta h$ ) was integrated from the calorimetric heat flow signal ( $dh/dt$ ) using a straight baseline with help of the STARE software.

The  $T_g$ s of the intermediate materials were determined with the following procedure: i) isothermal curing at 45 °C until the first reaction comes to the end (270 min); ii) dynamic heating from –30 to 250 °C at 10 °C/min.

To monitor the dual-curing process and to quantitatively determine the degree of curing, a FTIR spectrometer Bruker Vertex 70 with an attenuated total reflection accessory with thermal control and a diamond crystal (Golden Gate Heated Single Reflection Diamond ATR Specac-Teknokroma) and equipped with a mid-band liquid nitrogen-cooled mercury-cadmium-telluride (MCT) detector was used. Real-time spectra were collected in absorbance mode with a resolution of 4  $\text{cm}^{-1}$  in the wavelength range 4000 to 600  $\text{cm}^{-1}$  averaging 20 scans for each spectrum. The first step of the dual-curing process was conducted at 45 °C. Real-time spectra of the UV photoinitiated 2nd stage were recorded at the same conditions previously detailed. The characteristic absorbance peak of the epoxy at 915  $\text{cm}^{-1}$  (epoxy bending) was used to monitor the conversion of the epoxy group during the epoxy-amine reaction [26]. The disappearance of the absorbance peak at 1636  $\text{cm}^{-1}$  corresponding to stretching of the C=C bond of the methacrylate was used to monitor the homopolymerization of this group (2nd stage) [27]. Absorbance of each scanned sample were normalized with that of the DGEBA's aromatic protons at 1600  $\text{cm}^{-1}$ . In the case of formulations without DGEBA the peak corresponding to the carbonyl group of the methacrylate at 1718  $\text{cm}^{-1}$  was taken as the reference. Epoxy groups conversion ( $X_{\text{epoxy}}$ ) and methacrylate group conversion ( $X_{\text{meth}}$ ) were calculated by Eqs. (1) and (2), respectively

$$\chi_{\text{epoxy}} = 1 - \frac{A_{915}}{A_{915,0}} \quad (1)$$

$$\chi_{\text{meth}} = 1 - \frac{A_{1636}}{A_{1636,0}} \quad (2)$$

where  $A_{915}$  and  $A_{915,0}$  are the normalized absorbances of the epoxy peak at 915  $\text{cm}^{-1}$  at a given reaction time at the beginning of the curing process, respectively and  $A_{1636}$  and  $A_{1636,0}$  the normalized absorbances of the methacrylate peak at 1636  $\text{cm}^{-1}$  at the same given reaction time.

The gelation time was determined using a rheometer AR-G2 (TA Instruments) equipped with an electrical heated plate device (EHP) and 20 mm parallel plate geometry. The oscillation amplitude was set at 0.2% and the frequencies at 0.5, 1.75 and 3 Hz. Gel point was determined as the  $\tan \delta$  crossover at the three different frequencies. The evolution of the  $\tan \delta$  was monitored through dynamo-mechanical experiment at 45 °C during 4.5 h.

The thermomechanical properties were evaluated using DMA Q800 (TA Instruments) equipped with a three-point bending clamp. Prismatic rectangular samples of  $1.5 \times 5 \times 15 \text{ mm}^3$  were analysed from 25 to 150 °C at 1 Hz, 0.1% strain and with a heating rate of 3 °C/min.

TGA analyses were carried out with a Mettler Toledo TGA2 thermo-balance. Cured samples, weighting around 10 mg, were degraded between 30 and 600 °C at a heating rate of 10 °C/min in  $\text{N}_2$  atmosphere with a flow of 50  $\text{cm}^3/\text{min}$ .

### 3. Theoretical part

In non-isothermal kinetics of heterogeneous condensed phase reactions, it is usually accepted that the reaction rate is given by Eq. (3) [28,29].

$$\frac{d\alpha}{dt} = \beta \frac{d\alpha}{dT} = A \exp\left(-\frac{E}{RT}\right) f(\alpha) \quad (3)$$

where  $\alpha$  is the degree of conversion,  $T$  temperature,  $t$  time,  $f(\alpha)$  the differential conversion function,  $R$  the gas constant,  $\beta$  the linear constant heating rate  $\beta = dT/dt$  and  $A$  and  $E$  the pre-exponential factor and the activation energy given by the Arrhenius equation.

By integrating Eq. (3), in non-isothermal conditions, the integral rate equation, so-called temperature integral, may be expressed as Eq. (4).

$$g(\alpha) = \int_0^\alpha \frac{d\alpha}{f(\alpha)} = \frac{A}{\beta} \int_0^T e^{-(E/RT)} dT \quad (4)$$

where  $g(\alpha)$  is the integral conversion function.

By using the Coats-Redfern approximation to solve Eq. (4) and considering that  $2RT/E$  is much lower than 1, the Kissinger-Akahira-Sunose (KAS) equation (Eq. (5)) may be written [30–32]:

$$\ln\left(\frac{\beta}{T^2}\right) = \ln\left[\frac{AR}{g(\alpha)E}\right] - \frac{E}{RT} \quad (5)$$

For each conversion degree, the linear plot of  $\ln(\beta/T^2)$  versus  $T^{-1}$  enables  $E$  and  $\ln[AR/(g(\alpha)E)]$  to be determined from the slope and the intercept. Iso-conversional kinetic parameters were obtained in this work by using Eq. (5). If the reaction model,  $g(\alpha)$ , is known, the corresponding pre-exponential factor can be calculated for each conversion. Rearranging Eq. (5), the Coats-Redfern equation can be written as Eq. (6). [30,33].

$$\ln\left(\frac{g(\alpha)}{T^2}\right) = \ln\left[\frac{AR}{\beta E}\right] - \frac{E}{RT} \quad (6)$$

For a given model and heating rate, the linear plot of the left-hand side of Eq. (6) versus  $T^{-1}$  allowed us to obtain the average activation energy and average pre-exponential factor from the slope and the intercept. In this study, we chose the kinetic model with an activation energy similar to that obtained isoconversionally (Eq. (5)) and with a good correlation coefficient in Eq. (6) (Model Fitting method). The rate constant  $k$  and the reaction rate  $da/dt$  were calculated for each conversion from non-isothermal  $E$ , and  $A$  data using the Arrhenius equation and Eq. (3) and the kinetic model, respectively. Integrating Eq. (3) for

isothermal experiments, we can obtain Eq. (7):

$$\ln(t) = \ln \left[ \frac{g(\alpha)}{A} \right] + \frac{E}{RT} \quad (7)$$

This equation relates, for each conversion, the temperature and the time of curing. The constant  $\ln [g(\alpha)/A]$  is directly related to the value  $\ln [AR/(g(\alpha) E)]$  by  $E/R$ , which can be deduced from the non-isothermal adjustment (Eq. (5)), if isothermal and non-isothermal curing take place in the same conditions. In this work we used  $\ln [AR/(g(\alpha) E)]$  and  $E/R$  obtained by dynamic experiments and (Eq. (5)) to estimate the time of curing for both curing stages by using Eq. (7).

## 4. Results and discussion

### 4.1. Study of the curing process by calorimetry

With the aim to know the most adequate composition for the dual-curing process, we firstly studied the epoxy-amine reaction (1st stage) using GMA with structurally different amines (IPDA, TREN, JEFFA, and DETA) by means of DSC dynamic studies. Fig. 1 shows the curing exotherms obtained.

We can observe that the reactions with IPDA and JEFFA start at higher temperatures than with TREN and DETA. As it has been said, the thermal dual-curing includes a second stage which consists in a radical homopolymerization of the GMA methacrylate, which is initiated when Luperox decompose forming radical species close to 120 °C. Accordingly, the lower the starting temperature for the epoxy-amine reaction, the better to get sequentiality in the curing process. Moreover, the curing exotherms of TREN and DETA formulations are monomodal which may indicate that side reactions do not take place. Fig. 1 also shows, for TREN and DETA formulations, that the whole reaction has been completed between 30 °C and 170 °C and the reaction is fast once initiated.

Table 2 collects the most characteristic calorimetric data of the reactions studied in terms of reaction enthalpy ( $\Delta H$ ) and temperature of the maximum of exothermic peak ( $T_{max}$ ). As we can see, all reaction heats are relatively close to 90–100 kJ/eq, which is the standard value for an epoxy-amine reaction [34]. We can observe that IPDA releases a higher enthalpy than the other amines, but the peak appears at high temperature with a shoulder, which could indicate the presence of a homopolymerization of epoxides. According to these results, both TREN and DETA could be selected as curing agents for the epoxy-amine reaction in these formulations. Nevertheless, TREN contains a tertiary

amine that can act as a catalyst for aza-Michael addition between the methacrylate and the amine itself, hypothesis that we could confirm by FTIR analysis (Fig. S1). The absorbance peak corresponding to the double bond of the methacrylate at  $1636 \text{ cm}^{-1}$  decreased at the same time as the peak at  $915 \text{ cm}^{-1}$  of the epoxide at 45 °C, suggesting that the aza-Michael addition was taking place simultaneously with the epoxy-amine condensation. With these results we selected DETA as the amine to continue our study.

Once the amine is chosen, the initiator required to perform the second step must also be selected. According to Fig. 1 the epoxy-amine reaction embraces a big range of temperatures so it will be difficult to obtain a great sequentiality because many thermal radical initiators generate their radicals between 50 and 120 °C. Therefore, an initiator that releases its radicals at high temperature is needed to produce the epoxy-amine condensation and the homopolymerization of the methacrylate as the first and second curing stage, respectively. Among many thermal radical initiators like di-*tert*-butyl peroxide (TBP), 2,2'-azobisisobutyronitrile (AIBN), benzoyl peroxide etc. we selected 1,1-di(*t*-amylperoxy)-cyclohexane (Luperox 531 M60, Luperox or Lup hereafter) as the thermal radical initiator for the homopolymerization of the methacrylate moiety of the GMA because it generates radicals at 120 °C [35]. To test this initiator, a dynamic DSC scan was carried out for the formulation G\_DETA\_Lup which is shown in Fig. 2.

As it can be seen, the green curve presents a small shoulder at 110 °C corresponding to the maximum peak of the epoxy-amine condensation and then a high peak at 120 °C attributable to the homopolymerization of the methacrylate groups. Moreover, the global reaction heat was 128.1 kJ/eq., but taking into account that the epoxy-amine reaction releases 87.5 kJ/eq. the second step has 40.6 kJ/eq. which is a little bit lower than the standards for the methacrylate homopolymerization.

It is worth saying that GMA-amine formulations cannot gel during the first stage of the dual-curing, due to the monofunctionality of GMA in the epoxy-amine reaction, so that they produce a viscous liquid intermediate. Thus, to get a gelled intermediate material the addition of DGEBA, with a functionality of two, is necessary to get crosslinking points when amines have reacted. To investigate the amount of DGEBA needed to get gelation, the theoretical conversion of the epoxy groups at the gel point,  $\alpha_{gel}$ , during the epoxy-amine condensation had to be calculated assuming the ideal random step-wise reaction, using the well-known Flory-Stockmayer equation (Eq. (8)) [36,37]:

$$\alpha_{gel,theor} = \frac{r_1 f_1 - 1}{f_2 - 1} \quad (8)$$

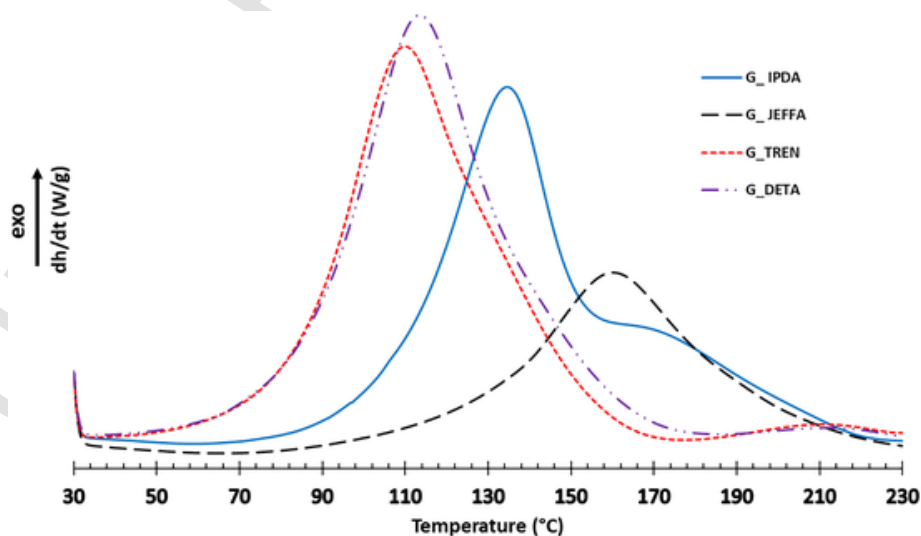


Fig. 1. DSC thermograms corresponding to the dynamic curing at 10 °C/min of formulations with GMA and the different amines.

**Table 2**  
Calorimetric data of the epoxy-amine reaction using different amines.

Sample	$\Delta H_{\text{epoxy-amine}}^a$ (J/g)	$\Delta H_{\text{epoxy-amine}}^a$ (kJ/eq)	$T_{\text{max}}^b$ (°C)
G_JEFFA	292.2	73.1	160.2
G_DETA	496.7	81.0	113.5
G_TREN	504.5	84.0	110.0
G_IPDA	497.5	92.2	134.5
GDG_DETA	478.9	87.5	106.7

<sup>a</sup> Enthalpy released in the epoxy-amine process by gram of mixture and by equivalent of epoxy.

<sup>b</sup> Temperature of the maximum of the exotherm of the epoxy-amine reaction.

where  $r$  is the hydrogen amine/epoxy equivalent ratio,  $f_1$  the epoxy monomer functionality and  $f_2$  the amine functionality.

With this equation, a ratio of nDGEBA/mGMA = 0.166 was calculated as the lowest to achieve the gelation at 100% of conversion. Two different possibilities were studied herein: a) a ratio nDGEBA/mGMA = 0.4, in which gelation will be achieved before full conversion to obtain a conformable solid-intermediate material and b) a ratio nDGEBA/mGMA = 0, where gelation will not occur and a viscous liquid will be obtained.

Fig. 2 shows that the addition of DGEBA to the formulation accelerates the epoxy-amine reaction and a better splitting of both stages is observed although they are partially overlapped. In this formulation,

the maximum of the epoxy-amine exotherm appears at about 105 °C, whereas the methacrylate homopolymerization reaches its maximum at about 120 °C, because of the formation of radicals at this temperature. As it can be observed in Table 2, in formulations with or without DGEBA,  $\Delta H_{\text{epoxy-amine}}$  and  $T_{\text{max}}$  are very similar, but with a slightly higher enthalpy and a slightly lower temperature of the maximum for GDG\_DETA, facilitating the separation of the first and the second stages.

Although sequentiality cannot be reached in dynamic scans, it must be considered that in a technological process, each step of curing requires a different temperature to be completed without overlapping them. To find out these appropriate temperatures we perform kinetic studies of both stages separately.

To obtain the kinetic parameters of the epoxy-amine reaction, dynamic DSC experiments were performed. Fig. 3a and b show the DSC thermograms and the plot of the conversion against temperature, respectively for the epoxy-amine reaction of GDG\_DETA formulation at different heating rates (2.5, 5, 10 and 20 °C). These formulations did not contain the radical initiator to suppress acrylate homopolymerization. In Supporting Information, Fig. S2a and S2b report the same study for G\_DETA formulation.

As it can be observed, the temperature of the maximum of the exotherm is lower when the heating rate is slower, but in all cases the reaction heat remains constant with values between 87 and 87.9 kJ/eq, reaching almost 100% of conversion. The kinetic parameters of non-isothermal curing for GDG\_DETA formulation obtained by DSC experi-

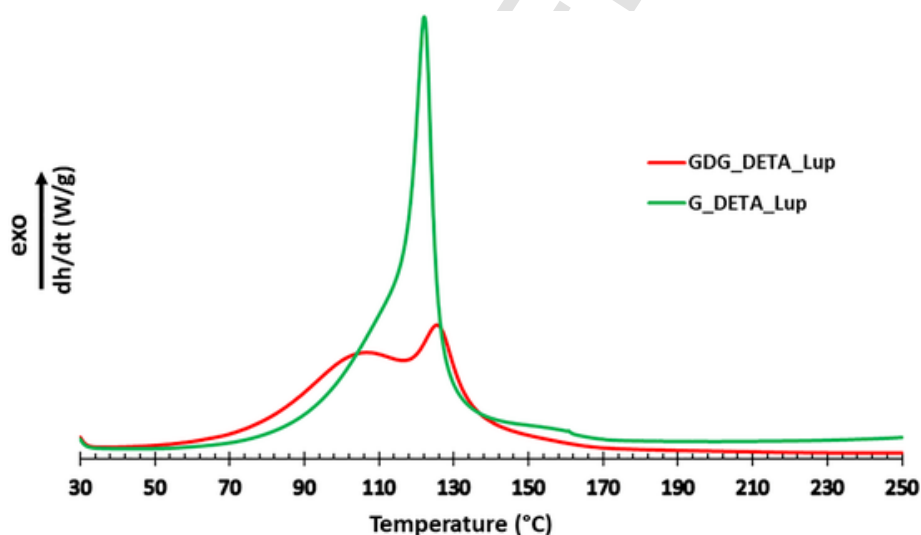


Fig. 2. DSC thermograms corresponding to the dynamic curing at 10 °C/min for GDG\_DETA\_Lup (red) and G\_DETA\_Lup (green) formulations. (For interpretation of the references to colour in this figure legend, the reader is referred to the web version of this article.)

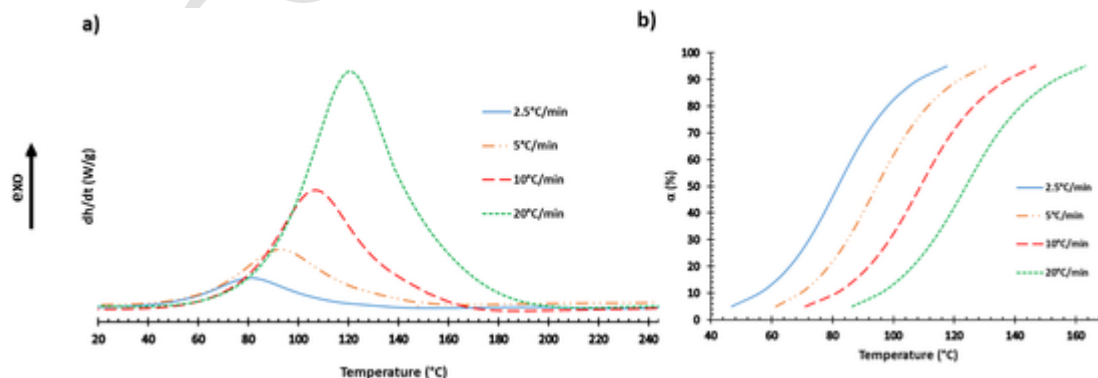


Fig. 3. a) DSC thermograms for the GDG\_DETA formulation at different heating rates and b) degree of conversion versus temperature for the same formulation.

ments are collected in Table 3 and for G\_DETA in Table S1. If we look in Table 3, it is possible to observe that the activation energy remains relatively constant in the process which indicates that the same mechanism is maintained in the whole reaction. Moreover, it suggests that a single kinetic model is needed to describe the curing. Furthermore, the reaction rate increases at low conversions but after reaching a maximum, decreases, confirming the autocatalytic behaviour of the epoxy-amine reaction. The hydroxyl groups formed during the epoxy-amine condensation catalyse the ring opening of the epoxides by forming hydrogen bonds between hydroxylic protons and the epoxides [38]. Moreover, the theoretical isothermal curing time for the first stage at 45 °C needed to achieve a 90% of conversion is 279 min, which is very

close to the reaction time in the oven that we obtained experimentally which was 270 min.

Once the first curing stage has been studied by DSC the characterization of the second stage is needed to optimize the global system. The standard reaction heat for a methacrylate homopolymerization is around 60 kJ/eq [39,40], and therefore it is important to verify the heat that the second curing stage releases after the epoxy-amine condensation. A dynamic DSC of the intermediate material prepared from GDG\_DETA\_Lup formulation, cured in the oven, gave us the  $T_g$  reached and the heat evolved by the homopolymerization while confirming that the first stage has been completed in the curing conditions determined by kinetic studies. Fig. 4a shows that the first stage has been completed giving a flexible solid material with a  $T_g = 14$  °C without the

**Table 3**  
Kinetic parameters from dynamic DSC studies of GDG\_DETA formulation.

$\alpha^a$	$E^b$ (kJ/mol)	$\ln[AR/g(\alpha)E]$ ( $K^{-1}\text{min}^{-1}$ )	$r^c$	$\ln A^d$ ( $\text{min}^{-1}$ )	$k^e$ ( $\text{min}^{-1}$ )	$d\alpha/dt^f$ ( $\text{min}^{-1}$ )	Isothermal time <sup>g</sup> (min)
0.05	45.5	6.44	0.991	13.77	0.032	0.009	8.52
0.1	47.51	6.66	0.998	14.47	0.031	0.010	14.12
0.15	48.53	6.71	0.999	14.82	0.029	0.014	19.42
0.2	49.20	6.71	0.999	15.05	0.029	0.012	24.63
0.3	50.06	6.66	0.999	15.34	0.028	0.009	35.20
0.4	50.71	6.61	0.999	15.58	0.028	0.008	46.68
0.5	51.40	6.60	0.999	15.83	0.027	0.007	60.44
0.6	52.19	6.62	0.999	16.11	0.027	0.005	78.78
0.7	53.08	6.64	0.999	16.41	0.026	0.003	106.51
0.8	53.91	6.56	0.999	16.68	0.025	0.002	155.46
0.9	55.31	6.48	0.999	17.11	0.022	0.001	279.31

<sup>a</sup> Conversion degree.

<sup>b</sup> Activation energy.

<sup>c</sup> Correlation coefficient.

<sup>d</sup> Pre-exponential factor calculated using kinetic the autocatalytic model.

<sup>e</sup> Rate constant calculated by Arrhenius equation.

<sup>f</sup> Reaction rate calculated by Eq. (3).

<sup>g</sup> Simulated isothermal time using non-isothermal isoconversional data.

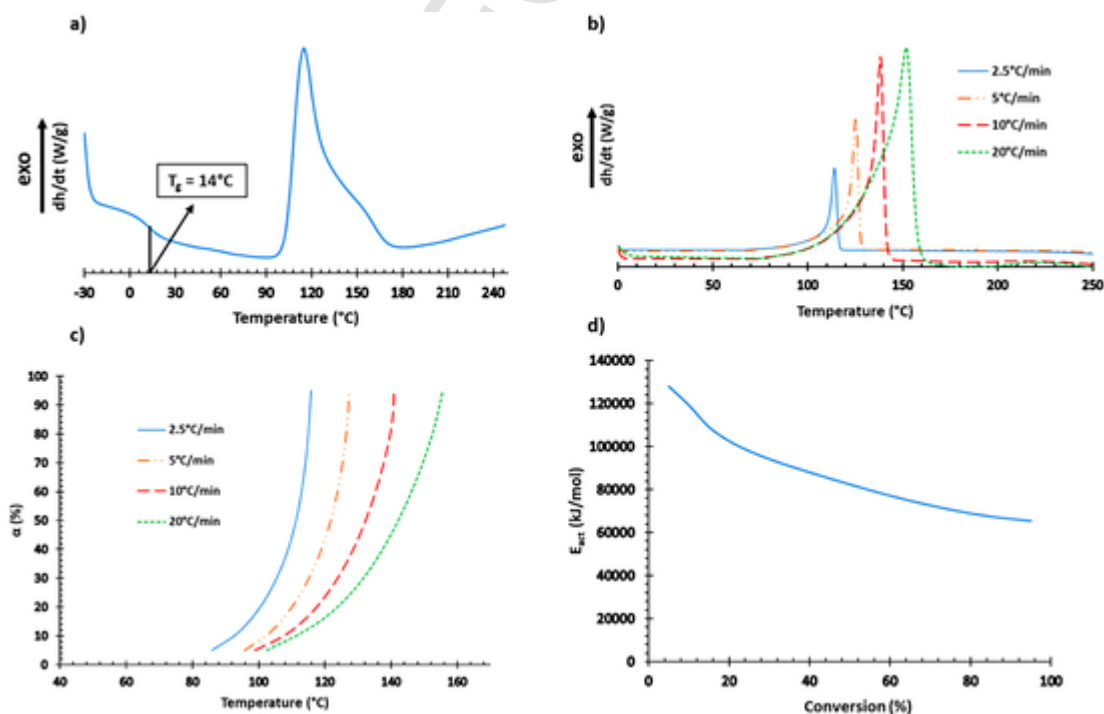


**Fig. 4.** a) DSC thermogram corresponding to the dynamic curing at 10 °C/min of the intermediate material for the formulation GDG\_DETA\_Lup, b) DSC thermograms for the second curing of a G\_Lup formulation at different heating rates, c) degree of conversion vs. temperature for the same sample and d) plot of activation energy versus conversion of the 2nd stage.



possibility to suffer dripping or exudation because no free unreacted molecules are present in the material. Moreover, we could check that the reaction heat released by the methacrylate homopolymerization was 41 kJ/eq. This value is lower than that reported, since not all methacrylate groups in the mixture will react due to topological restrictions, produced by the short distance between reactive groups in the GMA molecule. In the same way than for the 1st stage we determined the kinetic parameters by performing DSC experiments at the same heating rates to fully optimize the curing conditions.

The reaction heat in all the experiments remained relatively constant with values in the range 42.5–40.7 kJ/eq. Moreover, it can be seen in Fig. 4c that the conversion at the beginning increases slowly but rapidly gets higher values in a short range of temperatures, which can be attributed to the fast propagation once radicals are generated. If we look at the plot of the activation energy (Fig. 4d) we can see higher values at low conversions (initiation step) but a decrease when the conversion increases, due to the fact that termination, with a very low activation energy, begins to occur. The kinetic parameters of non-isothermal curing for the second stage obtained by DSC dynamic experiments are reported in Table S2. The higher activation energy of methacrylate homopolymerization in comparison to the epoxy-amine condensation puts in evidence the dual nature of the curing process.

The intermediate materials obtained after performing the 1st stage in the oven were stable at least for 4 days, since the  $T_g$  of this material remained unchanged, such as expected from the stability of the radical initiator at temperatures lower than 120 °C.

The thermomechanical characterization of this intermediate material was done and the obtained DMTA curves are represented in Fig. S3, where a maximum of  $\tan \delta$  of 23.5 °C and an storage modulus around 50 MPa at room temperature was determined. As expected, the modulus increases when the second curing stage initiates.

#### 4.2. Study of the curing process by FTIR spectroscopy

DSC provides information of the whole process but not about the evolution of the chemical reactions that occurs during curing. To get structural information, FTIR spectroscopy was applied to the isothermal curing of the reaction mixture. This methodology allows to determine the progress of the conversion at different reaction times for the functional groups involved in the reaction, taking as reference an invariable

absorption band. In addition, it gives information of the chemical structure of the network formed. Fig. 5 shows the evolution of the epoxy bands during the reaction for the GDG\_DETA mixture, which corresponds to the first stage of curing.

As it can be clearly seen, at 3400  $\text{cm}^{-1}$  an increase of the peak corresponding to the OH groups formed by the ring opening of the epoxide by the amine is taking place during the whole reaction time, while the band corresponding to the epoxy groups at 910  $\text{cm}^{-1}$  is declining, until complete disappearance, leading to the conclusion that the reaction has been completed during the curing process. Moreover, the band of the double bond of the methacrylate group at 1636  $\text{cm}^{-1}$  does not suffer any change, confirming that the methacrylate does not react in these conditions. The small band at 1636  $\text{cm}^{-1}$  attributed to the aromatic signals of DGEBA is maintained during the curing process and has been used as internal reference for kinetic studies.

Fig. S4 shows the FTIR conversion plot during isothermal curing at 45 °C (epoxy-amine reaction) for the GDG\_DETA sample (blue curve). We can see that the process starts relatively slowly at this temperature, which is in accordance with the calorimetric studies (red curve). The aforementioned autocatalytic character leads to an increased curing rate. Although the conversion reaches 90% in about 150 min, it takes a few more minutes to complete the reaction.

FTIR analysis was also applied to evaluate the conversion achieved in the second step of the curing process in both thermal and photochemical conditions. Fig. 6 present the FTIR spectra of the cured materials, when the homopolymerization of acrylates was initiated by Luperox (thermal) and DMPA (photochemical). The spectrum of the intermediate material has been added to visualize the changes produced.

After homopolymerization the absorption at 1636  $\text{cm}^{-1}$ , corresponding to the C=C st. of the methacrylate groups, has completely disappeared in case of GDG\_DETA\_Luperox formulation after heating at 120 °C, 150 °C and 200 °C during 90 min, 60 min and 90 min respectively indicating a full conversion of these groups and a complete curing. On the contrary for GDG\_DETA\_DMPA formulation there is still a small peak after long irradiation times (1.5 min at room temperature), which indicates that some methacrylic groups remain unreacted after long irradiation times. This observation leads us to conclude that vitrification has occurred when irradiating, hindering the achievement of a complete reaction at these temperature conditions, which will affect the final performance of this thermoset.

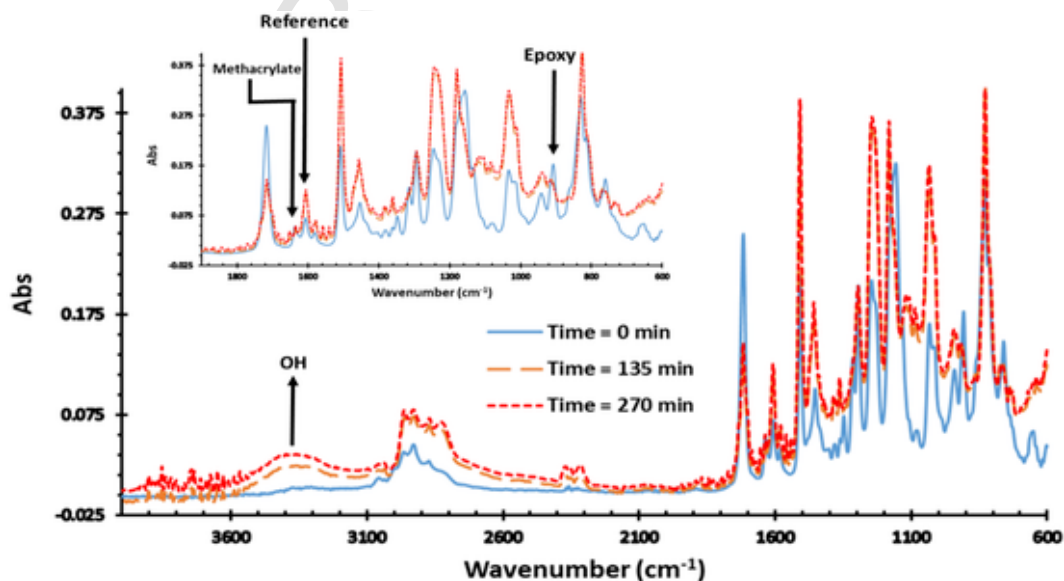


Fig. 5. Evolution of FTIR spectra at 45 °C for GDG\_DETA monitored during 270 min.

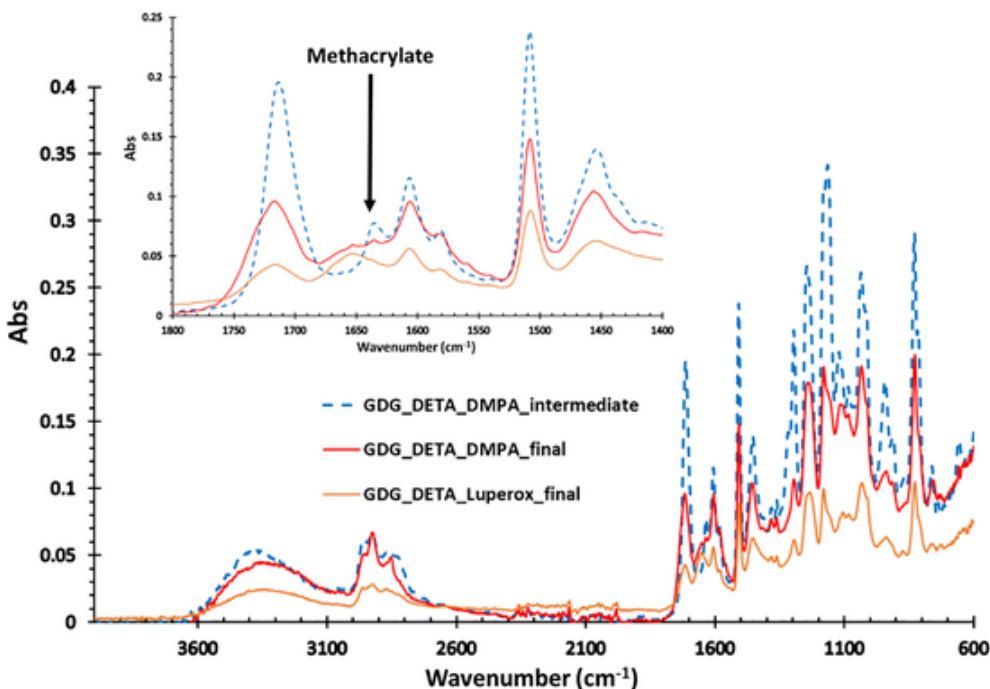


Fig. 6. FTIR spectra of the intermediate material (blue line) and of the final thermosets obtained in thermal (orange line) or in photochemical conditions (red line). (For interpretation of the references to colour in this figure legend, the reader is referred to the web version of this article.)

### 4.3. Study of the gelation process by rheology

As mentioned before, the addition of DGEBA to the GMA formulation enables the system to achieve the gelation during the 1st stage. At the gelation point there is a change of liquid to solid behaviour and the gelled material can be processed by different manufacturing processes like, for example, compression moulding.

To determine the gel time, rheology is the best methodology among those used. Rheometric measurements were carried out for G\_DETA and GDG\_DETA formulations to compare the behaviour of both compositions and to find out the gelation time of the latter. Fig. 7 shows the plot of  $\tan \delta$  vs. time for GDG\_DETA formulation at three different frequencies. The point at which the three  $\tan \delta$  intersect corresponds to the gelation time, which was 88 min at 45 °C. Fig. S5 shows the same graph for the G\_DETA formulation in which we can see that the  $\tan \delta$

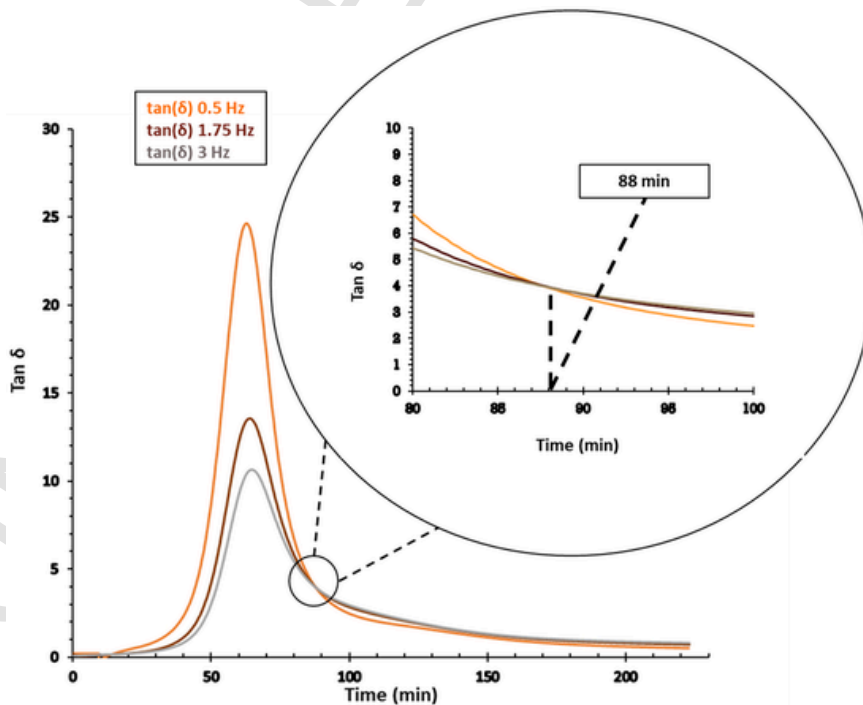


Fig. 7. Evolution at 45 °C of  $\tan \delta$  vs. time at three different frequencies for GDG\_DETA formulation.



curves do not intersect at any point in the whole process indicating that no gelation occurs and, consequently, a viscous liquid will be obtained as the intermediate material, which can be applied on surfaces as adhesive or coating. Both intermediate materials will improve their mechanical performance once the 2nd stage has been completed.

Rheological experiments by themselves do not allow to determine the conversion at the gelation for the GDG\_DETA formulation, but this value can be calculated from the conversion evolution obtained by isothermal DSC or FTIR at 45 °C for 4.5 h (Fig. S4). In this figure it is possible to see that at 88 min the epoxy group has reached a conversion of about 70%, which fits quite well with the ( $\alpha_{gel}^{theor}$ ) calculated by Eq. (8), 75%.

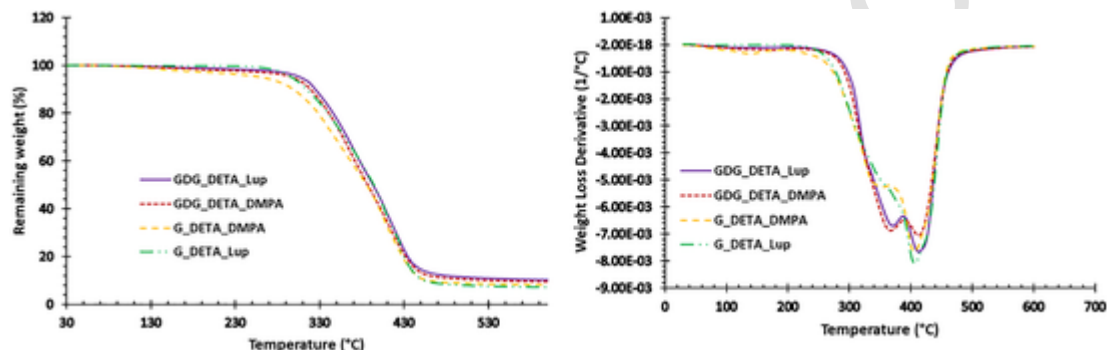


Fig. 8. TGA and DTGA curves for all the thermosets prepared in thermal and photochemical conditions in N<sub>2</sub> atmosphere.

Table 4  
Thermogravimetric and thermomechanical data of the thermosets prepared.

Sample	$T_{5\%}$ <sup>a</sup> (°C)	$T_{max}$ <sup>b</sup> (°C)	Char Yield <sup>c</sup> (%)	$T_{tan \delta}$ <sup>d</sup> (°C)	$E'_{glassy}$ <sup>e</sup> (MPa)	$E'_{rubbery}$ <sup>f</sup> (MPa)
GDG_DETA_Lup	307.3	368.5/412.8	10.3	168.4	3209	199.6
G_DETA_Lup	295.0	362.1/406.7	9.0	127.7	–	–
GDG_DETA_DMPA	297.9	366.7/411.5	9.7	100.7	3541	78.3
G_DETA_DMPA	261.2	354.6/405.9	9.1	97.8	–	–

<sup>a</sup> Temperature of 5% of weight loss.

<sup>b</sup> Temperature of the maximum rate of degradation of the two main steps.

<sup>c</sup> Char residue at 600 °C.

<sup>d</sup> Temperature at the maximum of  $\tan \delta$  peak at 1 Hz.

<sup>e</sup> Glassy storage modulus determined by DMTA.

<sup>f</sup> Rubbery storage modulus determined by DMTA.

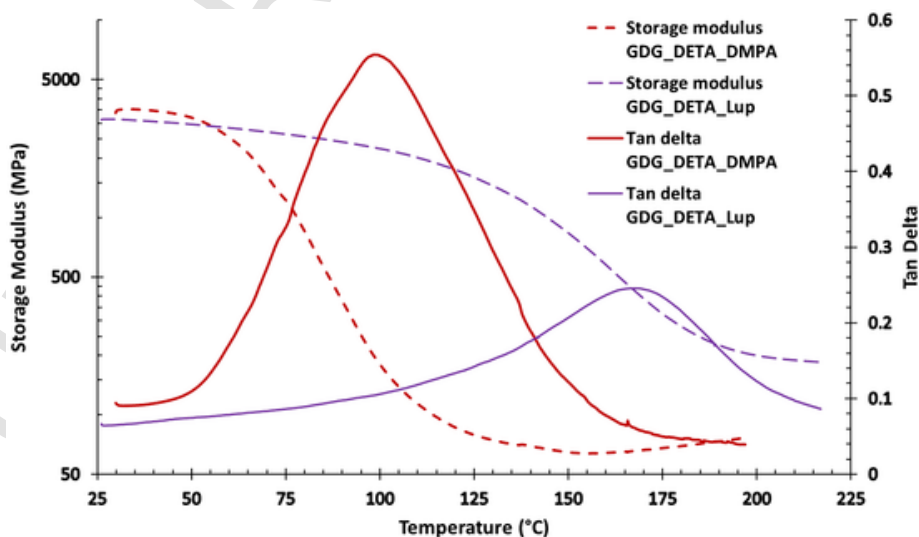


Fig. 9. Evolution of  $\tan \delta$  and storage modulus against temperature of GDG\_DETA\_Lup and GDG\_DETA\_DMPA thermosets.

at the temperature range of 270–370 °C can be assigned to the degradation of the poly(hydroxy-amine) network because of the high content of labile C—N bonds. The second step between 390 and 430 °C can be related to the poly(methacrylate) breakage [41]. The presence of aromatic moieties in the DGEBA containing thermosets leads to a slightly higher char yield.

The thermomechanical behaviour of both materials prepared was evaluated by DMTA analyses. Fig. 9 presents the  $\tan \delta$  curves as well as the storage modulus obtained for GDG\_DETA\_Lup and GDG\_DETA\_DMPA cured materials and the most representative data are collected in Table 4. The cured materials without DGEBA result in brittle and defective samples and the moduli could not be determined accurately enough (because the non-uniform dimensions) so they are not shown.

As we can see, the glassy moduli are similar and high for thermally and photochemically cured thermosets indicating the high rigidity of these materials at room temperature. The temperature at the  $\tan \delta$  peak is related to the glass transition temperature of the materials, and if we compare both values, we can observe a big difference of about 70 °C between them. This difference can be attributed to the vitrification of GDG\_DETA\_DMPA that takes place during UV-curing, since the temperature of curing is lower than its  $T_g$ . Due to vitrification, the photo-cured formulation is only partially cured, as we saw by FTIR, with lower crosslinking density, which is also reflected by its lower modulus in the rubbery state.

## 5. Conclusions

In this work, a new dual-cure system has been developed based on the joint presence of epoxy and methacrylate groups in a commercially available compound, glycidyl methacrylate. The first curing stage is a stoichiometric epoxy-amine condensation with the addition or not of DGEBA and the second, a free radical polymerization of methacrylate groups, thermally or UV-initiated.

The curing kinetics of both thermally induced stages have been studied by non-isothermal isoconversional analysis using DSC and monitored by real time FTIR analysis. Although dynamic DSC studies on complete formulations show that epoxy-amine and methacrylate homopolymerization processes occur overlapped, an adequate temperature has been found to perform a sequential curing with two well-differentiated steps, with the formation of a stable intermediate material. Depending on the radical initiator selected for the formulation, the second stage can be carried out in thermal or photochemical conditions.

The intermediate materials can be a deformable rubbery solid or a viscous liquid, depending on the addition or not of diglycidylether of bisphenol A to the reactive formulation. They have high stability and no dripping or exudation will take place as no unreacted monomers are present. The appropriate selection of the formulation composition allows to tailor the characteristics of the intermediate and final materials.

The final thermosets have a high glassy storage modulus which indicates their high rigidity at room temperature. Thermally cured materials have a higher glass transition temperature and crosslink density than the photo-cured ones, due to the vitrification of the latter. Despite this, the glass transition temperature exhibited by UV-cured material is high enough for most applications of interest. All these above-mentioned features together with the great thermal stability of the prepared materials open the possibility of working with them in applications that require high temperatures.

## CRediT author statement

A. Roig conducted the experiments and write the initial draft; X. Ramis and S. De la Flor developed methodology and S. De la Flor and A. Serra supervised and revised and edited the final version.

## Declaration of Competing Interest

There is no conflict of interest to declare.

## Acknowledgments

The authors would like to thank MINECO (Ministerio de Economía, Industria y Competitividad, MAT2017-82849-C2-1-R and 2-R) and Generalitat de Catalunya (2017-SGR-77 and BASE3D) for their financial support. Miwon Spain S.L. is thanked for donating glycidyl methacrylate.

## Appendix A. Supplementary data

Supplementary data to this article can be found online at <https://doi.org/10.1016/j.reactfunctpolym.2021.104822>.

## References

- [1] X. Luo, P.T. Mather, Shape memory assisted self-healing coating, *ACS Macro Lett.* 2 (2013) 152–156.
- [2] J. Verrey, M.D. Wakeman, V. Michaud, J.A.E. Månson, Manufacturing cost comparison of thermoplastic and thermoset RTM for an automotive floor pan, *Compos. Part A* 37 (2006) 9–22.
- [3] M. Giordano, A. Laudati, M. Russo, J. Nasser, G.V. Persiano, A. Cusano, Advanced cure monitoring by optoelectronic multifunction sensing system, *Thin Solid Films* 450 (2004) 191–194.
- [4] X. Ramis, X. Fernández-Francos, S. De La Flor, F. Ferrando, À. Serra, Click-based dual-curing thermosets and their application, in: Q. Guo (Ed.), *Structure, Properties and Application*, Ch.16, Thermosets second ed., Elsevier, 2018, pp. 511–541.
- [5] F. Gamardella, V. Sabatini, X. Ramis, À. Serra, Tailor-made thermosets obtained by sequential dual-curing combining isocyanate-thiol and epoxy-thiol click reactions, *Polymer* 174 (2019) 200–209.
- [6] S. Chatani, C. Wang, M. Podgórski, C.N. Bowman, Triple shape memory materials incorporating two distinct polymer networks formed by selective Thiol-Michael addition reactions, *Macromolecules* 47 (2014) 4949–4954.
- [7] K. Chen, X. Kuang, V. Li, G. Kang, H.J. Qi, Fabrication of tough epoxy with shape memory effects by UV-assisted direct-ink write printing, *Soft Matter* 14 (2018) 1879–1886.
- [8] A. Belmonte, C. Russo, V. Ambrogi, X. Fernández-Francos, S. De La Flor, Epoxy-based shape-memory actuators obtained via dual-curing of off-stoichiometric “thiol-epoxy” mixtures, *Polymers* 9 (2017) 113–131.
- [9] X. Zhang, L. Cox, Z. Wen, W. Xi, Y. Ding, C.N. Bowman, Implementation of two distinct wavelengths to induce multistage polymerization in shape memory materials and nanoimprint lithography, *Polymer* 156 (2018) 162–168.
- [10] S.H. Cho, S.R. White, P.V. Braun, Self-healing polymer coatings, *Adv. Mater.* 21 (2009) 3308–3313.
- [11] C.-H. Park, S.-W. Lee, J.-W. Park, H.-J. Kim, Preparation and characterization of dual curable adhesives containing epoxy and acrylate functionalities, *React. Funct. Polym.* 73 (2013) 641–646.
- [12] V.S. Khire, Y. Yi, N.A. Clark, C.N. Bowman, Formation and surface modification of nanopatterned thiol-ene substrates using step and flash imprint lithography, *Adv. Mater.* 20 (2008) 3308–3313.
- [13] A.M. Prenen, J.C.A. van der Werf, C.W.M. Bastiaansen, D.J. Broer, Monodisperse, polymeric nano- and microsieves produced with interference holography, *Adv. Mater.* 21 (2009) 1751–1755.
- [14] H. Peng, D.P. Nair, B.A. Kowalski, W. Xi, T. Gong, C. Wang, M. Cole, N.B. Cramer, X. Xie, R.R. McLeod, C.N. Bowman, High performance graded rainbow holograms via two-stage sequential orthogonal thiol-click chemistry, *Macromolecules* 47 (2014) 2306–2315.
- [15] W. Xi, H. Peng, A. Aguirre-Soto, C.J. Kloxin, J.W. Stansbury, C.N. Bowman, Spatial and temporal control of thiol-Michael addition via photocaged superbase in photopatterning and two-stage polymer networks formation, *Macromolecules* 47 (2014) 6159–6165.
- [16] N.B. Cramer, C.L. Couch, K.M. Schreck, J.E. Boulden, R. Wydra, J.W. Stansbury, C.N. Bowman, Properties of methacrylate-thiol-ene formulations as dental restorative materials, *Dent. Mater.* 26 (2010) 799–806.
- [17] J.E. Moses, A.D. Moorhouse, The growing applications of click chemistry, *Chem. Soc. Rev.* 36 (2007) 1249–1262.
- [18] W.H. Binder, R. Sachsenhofer, “Click” chemistry in polymer and materials science, *Macromol. Rapid Commun.* 28 (2007) 15–54.
- [19] H.C. Kolb, M.G. Finn, K.B. Sharpless, Click chemistry: diverse chemical function from a few good reactions, *Angew. Chem. Int. Ed.* 40 (2001) 2005–2021.
- [20] O. Konuray, X. Fernández-Francos, S. de la Flor, X. Ramis, À. Serra, The use of click-type reactions in the preparation of thermosets, *Polymers* 12 (2020) 1084.

- [21] O. Konuray, N. Areny, J.M. Morancho, X. Fernández-Francos, À. Serra, X. Ramis, Preparation and characterization of dual-curable off-stoichiometric amine-epoxy thermosets with latent reactivity, *Polymer* 146 (2018) 42–52.
- [22] J.M. Morancho, X. Ramis, X. Fernández, J.M. Francos, O. Salla, À. Serra Konuray, Curing of off-stoichiometric amine-epoxy thermosets, *J. Therm. Anal. Calorim.* 133 (2018) 519–527.
- [23] O. Konuray, A. García, J.M. Morancho, X. Fernández-Francos, À. Serra, F. Ferrando, M. García-Alvarez, X. Ramis, Hard epoxy thermosets obtained via two sequential epoxy-amine condensations, *Eur. Polym. J.* 116 (2019) 222–231.
- [24] K. Studer, C. Decker, E. Beck, R. Schwalm, Thermal and photochemical curing of isocyanate and acrylate functionalized oligomers, *Eur. Polym. J.* 41 (2005) 157–167.
- [25] F. Mustata, N. Tudorachi, I. Bicu, Thermosetting resins obtained via sequential photo and thermal crosslinking of epoxy resins. Curing kinetics, thermal properties and morphology, *Compos. Part B* 55 (2013) 470–478.
- [26] R. Thomas, C. Sinturel, J. Pionteck, H. Puliyalil, S. Thomas, In-situ cure and cure kinetic analysis of a liquid rubber modified epoxy resin, *Ind. Eng. Chem. Res.* 51 (2012) 12178–12191.
- [27] C. Russo, À. Serra, X. Fernández-Francos, S. De La Flor, Characterization of sequential dual-curing of thiol-acrylate-epoxy systems with controlled thermal properties, *Eur. Polym. J.* 112 (2019) 376–388.
- [28] S. Vyazovkin, *Isoconversional Kinetics of Thermally Stimulated Processes*, Springer, New York, NY, USA, 2015, pp. 166–231.
- [29] S. Vyazovkin, N. Sbirrazzuoli, Kinetic methods to study isothermal and nonisothermal epoxy-anhydride cure, *Macromol. Chem. Phys.* 200 (1999) 2294–2303.
- [30] A.W. Coats, J.P. Redfern, Kinetic parameters from thermogravimetric data, *Nature* 201 (1964) 68–69.
- [31] H.E. Kissinger, Reaction kinetics in differential thermal analysis, *Anal. Chem.* 29 (1957) 1702–1706.
- [32] R.L. Blaine, H.E. Kissinger, Homer Kissinger and the Kissinger equation, *Thermochim. Acta* 540 (2012) 1–6.
- [33] S. Vyazovkin, D. Dollimore, Linear and nonlinear procedures in isoconversional computations of the activation energy of non-isothermal reactions in solids, *J. Chem. Inf. Model.* 36 (1996) 42–45.
- [34] R.J. Varley, J.H. Hodgkin, D.G. Hawthorne, G.P. Simon, Toughening of a trifunctional epoxy system. II. Thermal characterization of epoxy/amine cure, *J. Appl. Polym. Sci.* 60 (1996) 2251–2263.
- [35] O. Konuray, F. Di Donato, M. Sangermano, J. Bonada, A. Tercjak, X. Fernández-Francos, À. Serra, X. Ramis, Dual-curable stereolithography resins for superior thermomechanical properties, *Express Polym Lett* 14 (2020) 881–894.
- [36] J.P. Pascault, H. Sautereau, J. Verdu, R.J.J. Williams, *Thermosetting Polymers*, Marcel Dekker, New York, 2002.
- [37] J.P. Pascault, R.J.J. Williams, Overview of thermosets: present and future, in: Q. Guo (Ed.), *Structure, Properties and Application*, Ch.11, *Thermosets 2nd ed.*, Elsevier, 2018, pp. 3–34.
- [38] B.A. Rozenberg, Kinetics, thermodynamics and mechanism of reactions of epoxy oligomers with amines, *Adv. Polym. Sci.* 75 (1986) 113–165.
- [39] A. Cadenato, J.M. Morancho, X. Fernández-Francos, J.M. Salla, X. Ramis, Comparative kinetic study of the non-isothermal thermal curing of bis-GMA/TEGDMA systems, *J. Therm. Anal. Cal.* 89 (2007) 233–244.
- [40] A.C. Uzcategui, A. Muralidharan, V.L. Ferguson, S.J. Bryant, R.R. McLeod, Understanding and improving mechanical properties in 3D printed parts using a dual-cure acrylate-based resin for stereolithography, *Adv. Eng. Mater.* 20 (2018) 1800876.
- [41] G. González, X. Fernández-Francos, À. Serra, M. Sangermano, X. Ramis, Environmentally-friendly processing of thermosets by two-stage sequential aza-Michael addition and free-radical polymerization of amine-acrylate mixtures, *Polym. Chem.* 6 (2015) 6987.6997.